brations are due to intermolecular vibrations. These intermolecular vibrations should be sought in the regions of 50–700 cm^{-1} and 20–500 cm^{-1} for $CH_3F{\cdot}HF$ and $CH_3Cl{\cdot}HCl$, respectively.

Finally, there is a real possibility of recording low-temperature vibrational spectra of the radical cation dimers of methane (V) and methyl fluoride (XII) in rigid inert matrices and to study gas-phase vibrational spectra of the $CH_3F{\cdot}HF$(XI) complex.[16] Computed vibrational frequencies and IR intensities are summarized for these species in Table VII. These frequencies have not been scaled, and therefore they are likely to be higher than the experimental values by 5–10%.[29]

(29) Hess, B. A., Jr.; Schaad, L. J.; Crsky, P.; Zahradnik, R. *Chem. Rev.* **1986**, *86*, 709.

Acknowledgment. Our thanks are due to Professor S. Suzuki (IMS, Okazaki) for drawing our attention to his recent studies of CH_3Cl^+ and for informing us about the reactivity of CH_3F^+ prior to publication. B.A.H. thanks the National Science Foundation for an instrument grant used to purchase an SCS-40 computer on which the calculations reported here were performed.

Supplementary Material Available: A table of SCF/6-31G** geometries, vibrational frequencies, and energies and MP2/6-31G**//MP2/6-31G** frequencies of I–XI, a table of SCF/6-31G**//SCF/6-31G** frequencies of XII–XVIII, a table of MP2-, MP3-, and MP4/6-31G**//MP2/6-31G** energies of I–XI, and a table of MP2-, MP3-, and MP4/6-31G**//SCF/6-31G** of XII–XVIII (8 pages). Ordering information is given on any current masthead page.

Penning Ionization Electron Spectroscopy of *n*-Alkane Ultrathin Films. Molecular Orbitals and Orientation of Molecules

Hiroyuki Ozaki*,† and Yoshiya Harada‡

Contribution from the Department of Chemistry, College of General Education, Nagoya University, Chikusa, Nagoya 464-01, Japan, and the Department of Chemistry, College of Arts and Sciences, The University of Tokyo, Komaba, Meguro, Tokyo 153, Japan.
Received October 30, 1989

Abstract: Penning ionization electron spectra (PIES) were measured for evaporated ultrathin films [4 (monolayer) to 200 Å thick] of long-chain *n*-alkanes. The electron distributions as well as the energies of three types of MOs (pseudo-π, σ_{2p}, and σ_{2s}), obtained by ab initio MO calculations, could be surveyed experimentally by PIES; the agreement between the calculated and experimental results was fairly good. The valence electronic structure of long-chain *n*-alkanes is characterized by the high density of states of the pseudo-π and σ_{2s} MOs, which were predominantly detected for monolayer films made up of flat-lying molecules. For crystalline films comprised of molecules standing upright, MOs with large distribution on the terminal hydrogen atom were exclusively detected. These data serve for the PIES characterization of various molecular aggregates of alkane derivatives, including Langmuir–Blodgett films. Ultraviolet photoelectron spectra were also measured, but unlike PIES, they were severely influenced by substrate signals and/or conduction band structures. It was demonstrated that Penning spectroscopy probes occupied orbitals selectively.

Introduction

n-Alkanes are among the most fundamental organic compounds, and their fragments, alkyl groups, are contained in many chemical substances. Furthermore, Langmuir–Blodgett (LB) films[1,2] and some polymers mainly consist of alkyl chains. To develop a molecular organism of an alkane derivative with a new function, the electronic structures of the constituent molecule must be elucidated. The electronic structure of long-chain *n*-alkanes has been studied as a model to simulate that of polyethylene.[3-9] Since the *n*-alkane having 13 carbons, tridecane, gave an X-ray photoelectron spectrum similar to that of polyethylene, 10 carbons or so were considered to be sufficient to simulate the infinite chain of polyethylene.[3,4] Therefore, the results of electron spectroscopic measurements for *n*-alkanes have been interpreted on the basis of band calculations for polyethylene.[5-8] We plan here, however, to show that the valence electronic structure of *n*-alkanes viewed with the molecular orbital picture can be explored experimentally by Penning ionization electron spectroscopy.

The kinetic energy analysis of electrons ejected by collisions between target molecules M and metastable rare gas atoms, e.g., He* (2^3S) with excitation energy 19.82 eV, ($M + He^* \rightarrow M^+ + He + e^-$) provides a Penning ionization electron spectrum (PIES).[10] In this ionization process, an electron in an MO of M transfers to the vacant 1s AO of He*, and an electron in the 2s AO of He* is ejected simultaneously to an orbital of the continuum state.[11] The process is illustrated for solid-phase molecules in Figure 1. Since metastables do not permeate into the solid and the transition probability is governed by the spatial overlap of the relevant MO and the helium 1s AO, an MO spreading outside the repulsive (van der Waals) surface of molecules in the outermost layer provides a stronger band in the PIES than an MO distributed inside the surface. Accordingly,

† Nagoya University.
‡ The University of Tokyo.

(1) Blodgett, K. B. *J. Am. Chem. Soc.* **1935**, *57*, 1007–1022.
(2) *Thin Solid Films* **1983**, *99*, 1–329.
(3) Pireaux, J. J.; Svensson, S.; Basilier, E.; Malmqvist, P.-Å.; Gelius, U.; Caudano, R.; Siegbahn, K. *Phys. Rev.* **1976**, *A14*, 2133–2145.
(4) Pireaux, J. J.; Caudano, R. *Phys. Rev.* **1977**, *B15*, 2242–2249.
(5) Seki, K.; Hashimoto, S.; Sato, N.; Harada, Y.; Ishii, K.; Inokuchi, H.; Kanbe, J. *J. Chem. Phys.* **1977**, *66*, 3644–3649.
(6) Seki, K.; Ueno, N.; Karlsson, U. O.; Engelhardt, R.; Koch, E. E. *Chem. Phys.* **1986**, *105*, 247–265, and references therein.
(7) Ueno, N.; Fukushima, T.; Sugita, K.; Kiyono, S.; Seki, K.; Inokuchi, H. *J. Phys. Soc. Jpn.* **1980**, *48*, 1254–1260.
(8) Ueno, N.; Sugita, K.; Kiyono, S. *Chem. Phys. Lett.* **1981**, *82*, 296–300.
(9) Hashimoto, S.; Seki, K.; Sato, N.; Inokuchi, H. *J. Chem. Phys.* **1982**, *76*, 163–172.
(10) Čermák, V. *J. Chem. Phys.* **1966**, *44*, 3781–3786.
(11) Hotop, H.; Niehaus, A. *Z. Phys.* **1969**, *228*, 68–88.

0002-7863/90/1512-5735$02.50/0

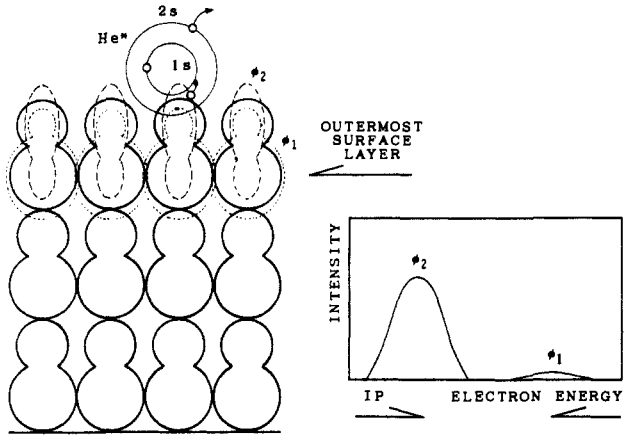

Figure 1. Penning ionization of a solid-phase molecule by a helium metastable atom He* (2^3S). An electron in an MO of a molecule in the outermost surface layer transfers to the vacant 1s AO of He*, and an electron in the 2s AO of He* is ejected simultaneously. MO ϕ_2 protruding outside interacts with He* more effectively and, hence, provides a more enhanced band in the PIES than MO ϕ_1 with little distribution outside the surface. The thick solid line indicates the molecular van der Waals surface.

the relative intensity of PIES bands indicates the local electron distribution of individual MOs (LEDMO) at the externally exposed portion of the molecular surface.[12-15] Applying this unique characteristic of PIES to vapor-deposited ultrathin films of planar organic compounds, we have investigated the electronic structure of the molecules[13-15] and also have obtained information on the aggregation of surface molecules: the process of epitaxial growth was observed layer by layer;[16] a thermally induced structural change in a monolayer was sensitively detected;[17] different molecular arrangements in films prepared under different conditions were discriminated.[13]

Another important characteristic of solid-phase PIES is that it reflects the valence electronic structure rather *faithfully*. This is not always the case for an ultraviolet photoelectron spectrum (UPS), which has been conventionally used to study the electronic structure of organic solids. The UPS of long-chain *n*-alkanes are known to be influenced severely by secondary electrons.[5] Photoelectrons produced in the solid suffer inelastic scattering during travel to the surface before they are emitted, which results in secondary electrons. They accumulate in unoccupied states having high densities to exhibit predominant features in the UPS. On the other hand, Penning electrons are directly excited to the continuum state at the surface (see Figure 1). Therefore, it is expected that more genuine features due to occupied MOs of long-chain *n*-alkanes are reflected in the PIES.

Recently, we initiated the characterization of LB films by PIES.[18,19] Though a knowledge of MOs (energy and shape) is necessary to study molecular orientation in such films, the MOs of a long-chain *n*-alkane (as a substitute for the alkyl chain) have not been well studied. There are no available data based on ab initio MO calculations for *n*-alkanes longer than nonane (C_9H_{20}).[3] Moreover, the character or the shape of each MO has not been given except in the case of very short chains.[20] In this paper, we present basic data for the characterization of alkyl-chain aggregates: the PIES and UPS of long-chain *n*-alkanes vapor-deposited onto a graphite substrate at low temperature and onto a metal substrate at room temperature. From our previous studies,[13-17] the molecules are expected to lie in the former case, but they are known to stand in the latter case,[5,9] which will be useful for probing the LEDMO by PIES at different molecular areas (the chain side and terminal). The results of ab initio MO calculations for several *n*-alkanes containing 10–19 carbons are also given. Comparing the experimental and calculated results, we examine the valence electronic structure from the LEDMO and provide the overall view of *n*-alkane MOs.

Experimental Section

The preparation of evaporated films and the measurement of PIES and UPS were carried out with an ultrahigh vacuum (base pressure less than 4×10^{-8} Pa) apparatus reported previously.[13] Three *n*-alkanes, hexacosane ($C_{26}H_{54}$), hexatriacontane ($C_{36}H_{74}$), and tetratetracontane ($C_{44}H_{90}$), were obtained commercially; only tetratetracontane was purified by recrystallization from benzene solution. Impurities with lower vapor pressure, however, were eliminated in the sample preparation chamber of the apparatus by heating the quartz sample boat to higher temperature than that used for film preparation. Two kinds of substrates were used: one is made of copper and the other is a piece of grafoil (10×14 mm^2, 0.4 mm thick) fastened with a copper wire to a stainless steel substrate. We will identify the latter as the graphite substrate, because grafoil consists of graphite crystallites with their cleavage planes oriented parallel to the foil plane.[21] The graphite substrate was cleaned by heating it to 570 K for 48 h and to 670 K for 48 h under ultrahigh vacuum. The copper substrate was also heated to 550 K for 36 h, but this substrate does not have a "clean", crystallographic surface. Both $C_{36}H_{74}$ and $C_{44}H_{90}$ were deposited onto the substrates after the preparation chamber was evacuated to 10^{-8} Pa by baking it as usual, but $C_{26}H_{54}$ was deposited at 10^{-6} Pa without baking because of the high vapor pressure of this alkane.

The amount of the deposited sample was monitored with a quartz oscillator, calibrated in advance, and was estimated as follows. On Pt(111)[22] and Ag(111) surfaces,[23] some short *n*-alkanes, C_4H_{10}–C_8H_{18}, form monolayer films in which molecules all in trans conformation pack closely with their planes of carbon skeleton parallel to the substrate surfaces. On the Pt(111) surface, the monolayer of an odd-numbered alkane contains one molecule per surface unit cell, while that of an even-numbered alkane contains two molecules per unit cell. Though the shapes of the unit cells differ between them, the formula giving the area of the substrate surface occupied by a molecule with carbon number N, $S(N)$, is the same for both cases and is given by

$$S(N) = 6.65(N + 1) \quad (\text{Å}^2/\text{molecule})$$

Monolayers formed on the Ag(111) surface have almost the same values of $S(N)$. Assuming that the equation holds for larger N such as 26, 36, and 44, we estimated the amount of alkane required to form a close-packed monolayer with flat molecular orientation, i.e., one *monolayer equivalence* (MLE).

Ultrathin films were prepared by depositing 1 MLE of alkanes onto the graphite substrate held at 213 K (films I) and several dozen MLE onto the copper substrate at room temperature (films II). The deposition rates for films I and II were 0.5 and 1 MLE/min, respectively. The film of $C_{26}H_{54}$, however, could not be formed on the copper substrate under these conditions. Thus, we obtained five specimens: films I_{26} ($C_{26}H_{54}$; 1 MLE), I_{36} ($C_{36}H_{74}$; 1 MLE), I_{44} ($C_{44}H_{90}$; 1 MLE), II_{36} ($C_{36}H_{74}$; 68 MLE), and II_{44} ($C_{44}H_{90}$; 34 MLE).[24] After the sample preparation, the substrate was transferred into the analyzer chamber and the PIES and UPS were measured. He* (2^3S, 19.82 eV) metastable atoms were used for PIES and the He I (21.22 eV) resonance line was used for UPS as

(12) Munakata, T.; Ohno, K.; Harada, Y. *J. Chem. Phys.* **1980**, *72*, 2880–2881.
(13) Harada, Y.; Ozaki, H. *Jpn. J. Appl. Phys.* **1987**, *26*, 1201–1214.
(14) Ozaki, H.; Harada, Y. *J. Am. Chem. Soc.* **1987**, *109*, 949–950.
(15) Ozaki, H.; Harada, Y. *J. Chem. Phys.* **1990**, *92*, 3184–3188.
(16) Harada, Y.; Ozaki, H.; Ohno, K. *Phys. Rev. Lett.* **1984**, *52*, 2269–2272.
(17) Harada, Y.; Ozaki, H.; Ohno, K.; Kajiwara, T. *Surf. Sci.* **1984**, *147*, 356–360.
(18) Ozaki, H.; Harada, Y.; Nishiyama, K.; Fujihira, M. *J. Am. Chem. Soc.* **1987**, *109*, 950–951.
(19) Harada, Y.; Hayashi, H.; Ozaki, H.; Kamata, T.; Umemura, J.; Takenaka, T. *Thin Solid Films* **1989**, *178*, 305–312.
(20) Kimura, K.; Katsumata, S.; Achiba, Y.; Yamazaki, T.; Iwata, S. *Handbook of HeI Photoelectron Spectra of Fundamental Organic Molecules*; Japan Scientic Societies Press: Tokyo, 1981.
(21) Kjems, J. K.; Passell, L.; Taub, H.; Dash, J. G.; Navaco, A. D. *Phys. Rev.* **1976**, *B13*, 1446–1462.
(22) Firment, L. E.; Somorjai, G. A. *J. Chem. Phys.* **1977**, *66*, 2901–2913.
(23) Firment, L. E.; Somorjai, G. A. *J. Chem. Phys.* **1978**, *69*, 3940–3952.
(24) Upon evaporation onto an "unclean" metal substrate at room temperature, long-chain *n*-alkanes form polycrystalline films in which molecules stand upright (see below). With this molecular orientation, at least 17 MLE of *n*-alkane is needed to cover the substrate, provided that it has a smooth surface. Since this is not the case and the film does not necessarily grow layer by layer,[13] more sample must be deposited to eliminate the substrate signals in the PIES and UPS. As the film becomes thicker, however, its charging affects the spectra. The deposited amounts of alkanes for films II were chosen so as to reduce the substrate features in the spectra and also to avoid the film charging.

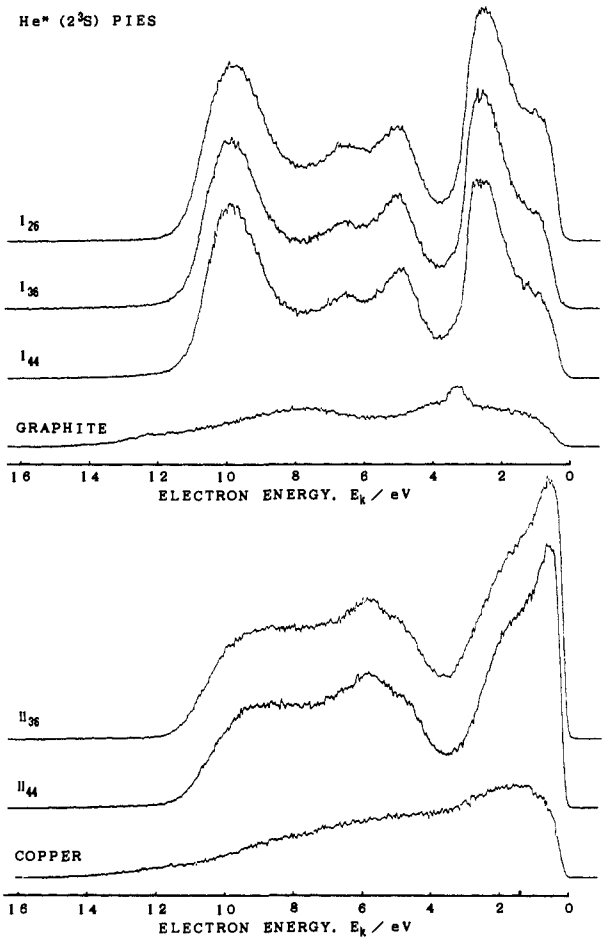

Figure 2. He* (2^3S, 19.82 eV) PIES of *n*-alkane evaporated films. Films I_{26}, I_{36}, and I_{44} were prepared by depositing 1 MLE (monolayer equivalence, the amount of the sample required to form a close-packed monolayer with flat molecular orientation) of hexacosane ($C_{26}H_{54}$), hexatriacontane ($C_{36}H_{74}$), and tetratetracontane ($C_{44}H_{90}$) on a graphite substrate at 213 K, respectively. Films II_{36} and II_{44} were formed by depositing 68 MLE of hexatriacontane and 34 MLE of tetratetracontane on a copper substrate at room temperature, respectively. The spectra of the graphite and copper substrates are also shown.

the excitation sources. The incidence angle of the He* metastable beam or the ultraviolet ray was 30° relative to the substrate surface normal, and the emission angle of electrons was 60°.

Calculation. Ab initio MO calculations were performed with an STO-3G basis set for all trans *n*-alkanes, decane ($C_{10}H_{22}$), tridecane ($C_{13}H_{28}$), hexadecane ($C_{16}H_{34}$), and nonadecane ($C_{19}H_{40}$).[25,26] The bond lengths and bond angles of hexadecane obtained by electron diffraction were used for the four compounds: C–C, 1.542 Å; C–H, 1.130 Å; ∠ C–C–C, 114.6°, ∠ C–C–H, 110.4°.[27]

Results and Discussion

The PIES of the *n*-alkane ultrathin films are shown in Figure 2 together with the substrate spectra. Every film gives a PIES completely different from the spectrum of the substrate on which it was formed. Since helium metastables do not penetrate into solid, this indicates that the substrate surface is covered with *n*-alkane molecules and that metastables interact with the outermost surface molecules selectively. Furthermore, the fact that features due to graphite are almost missing in the PIES of 1 MLE films I_{26}, I_{36}, and I_{44} means that these films are monolayers in which molecules lie flat, because the molecules would not cover the graphite surface in 1 MLE films if they stood or tilted on it. As will be discussed below, the flat molecular orientation in films

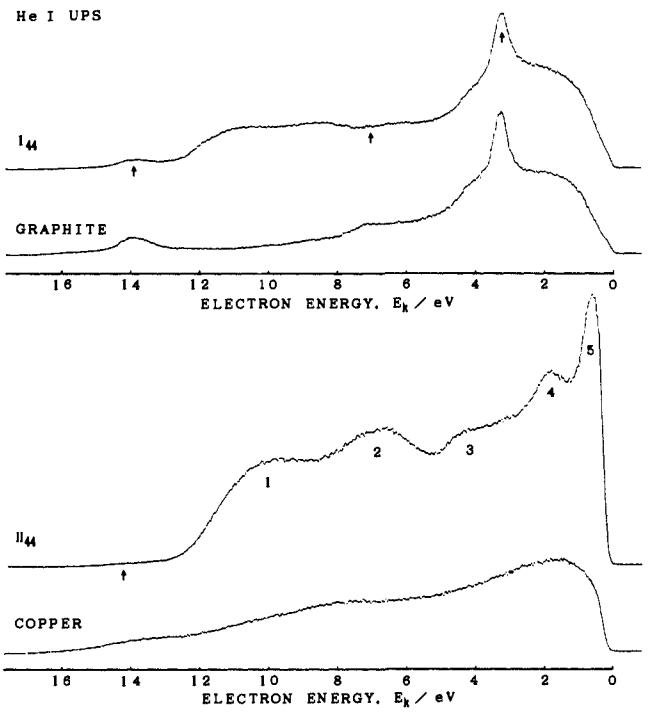

Figure 3. He I (21.22 eV) UPS of tetratetracontane films I_{44} and II_{44} together with those of the substrates. Features ascribed to the substrates are indicated by arrows in the film spectra.

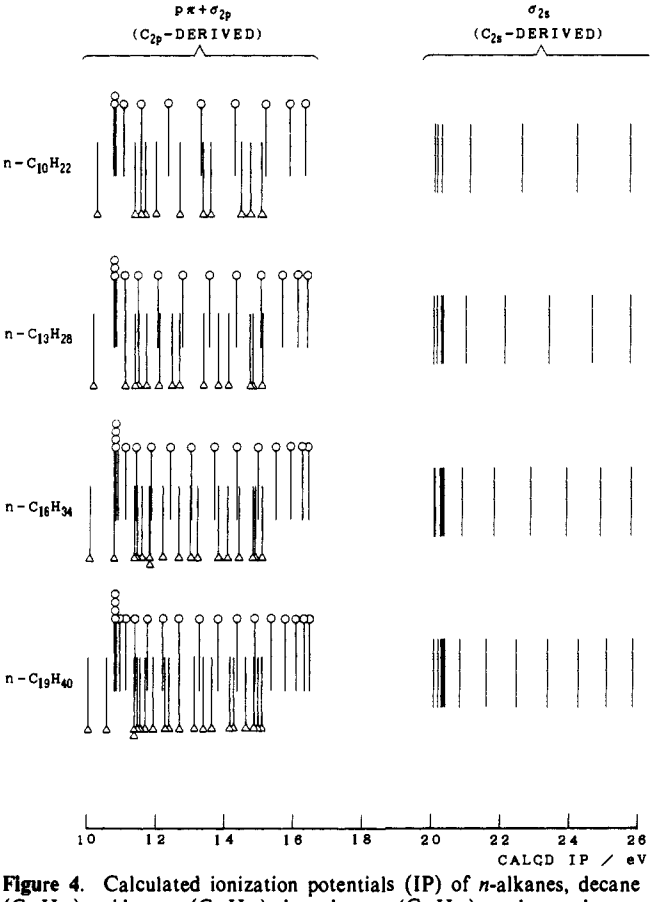

Figure 4. Calculated ionization potentials (IP) of *n*-alkanes, decane ($C_{10}H_{22}$), tridecane ($C_{13}H_{28}$), hexadecane ($C_{16}H_{34}$), and nonadecane ($C_{19}H_{40}$). Bars labeled with open circles and triangles correspond to pseudo-π (pπ) and σ_{2p} MOs, respectively, the other bars to σ_{2s} MOs.

I is also supported by the relative band intensity in the PIES. Another observation to note is that the PIES of different *n*-alkanes on the same substrate are almost the same: $C_{26}H_{54}$, $C_{36}H_{74}$, and $C_{44}H_{90}$ on graphite (films I); $C_{36}H_{74}$ and $C_{44}H_{90}$ on copper (films II). In contrast, the two films of the same compound formed on

(25) Hehre, W. J.; Stewart, R. F.; Pople, J. A. *J. Chem. Phys.* **1969**, *51*, 2657–2664.
(26) Kosugi, N. Program *GSCF2*, Program Library, The Computer Center, The University of Tokyo, 1981.
(27) Fitzwater, S.; Bartell, L. S. *J. Am. Chem. Soc.* **1976**, *98*, 8338–8344.

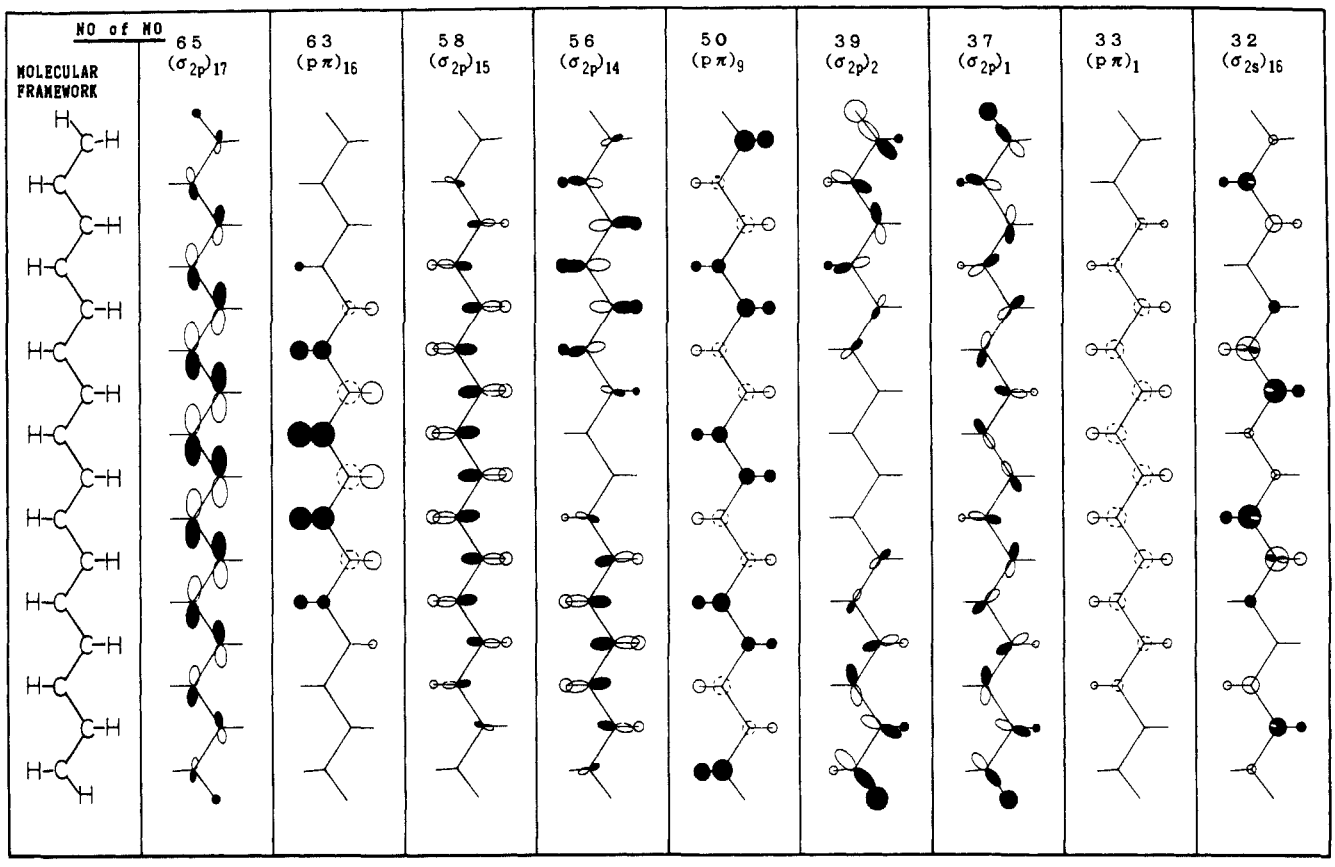

Figure 5. MO drawings of hexadecane. The constituent AOs of each MO are projected onto the plane of the carbon skeleton (*xy* plane). The sizes of AOs are proportional to the coefficients of the MO wave functions. The carbon $2p_x$ and $2p_y$ AOs are shown as their sums. The carbon $2p_z$ AOs are drawn as broken (or closed) circles, whereas the hydrogen 1s and carbon 2s AOs are drawn as full (or closed) circles. The 65, 63, and 32 MOs are the highest occupied σ_{2p} (also HOMO), $p\pi$, and σ_{2s}, respectively; 58 and 56 are σ_{2p} MOs with little distribution on the terminal hydrogen atom, whereas 39 and 37 are those with a large contribution from the terminal hydrogen 1s AO. In the first column, the molecular framework of hexadecane is shown.

different substrates give PIES entirely different from each other: films I_{36} and II_{36}; films I_{44} and II_{44}.

The UPS of the $C_{44}H_{90}$ films, I_{44} and II_{44}, and the substrates are shown in Figure 3. The UPS of other films were essentially the same as those of the $C_{44}H_{90}$ films formed on the same substrate, as in the case of the PIES. In the UPS of the films, features ascribed to the substrates (indicated by arrows) are observed, which means that photons pass through the ultrathin organic layers and interact with the substrates.[28] In particular, the UPS of the monolayer film I_{44} is influenced severely by electrons originating in graphite to exhibit the features characteristic of the *n*-alkane.

Figure 4 shows the calculated ionization potentials (IP) of the four *n*-alkanes via Koopmans' approximation. Some MOs of $C_{16}H_{34}$ are drawn in Figure 5. The constituent AOs of each MO are projected onto the plane of the carbon skeleton (*xy* plane); the sizes of the AOs are proportional to the coefficients of the MO wave functions. Carbon $2p_x$ and $2p_y$ AOs are shown as their sums. Carbon $2p_z$ AOs are drawn as broken (or closed) circles, whereas hydrogen 1s and carbon 2s AOs are drawn as full (or closed) circles. We can classify the MOs of *n*-alkane into three types, $p\pi$, σ_{2p}, and σ_{2s}. The $p\pi$ MOs (such as 63, 50, and 33 in Figure 5) consist of carbon $2p_z$ and hydrogen 1s AOs and, hence, have pseudo-π character, spreading almost perpendicularly to the carbon skeleton plane. The σ_{2p} MOs (e.g., 65, 58, 56, 39, and 37) are made up of carbon $2p_x$, $2p_y$ and hydrogen 1s AOs, while the σ_{2s} MOs (e.g., 32) are mainly composed of carbon 2s AOs. In Figure 4, the $p\pi$ and σ_{2p} MOs are labeled with open circles and triangles, respectively.

Each *n*-alkane in Figure 4 has an energy gap between IP 16.5 and 20.1 eV; $p\pi$ and σ_{2p} MOs are present above this energy gap and σ_{2s} MOs below it. In addition, some MO energies tend to gather around IPs of 11 and 20 eV as the alkyl chain becomes longer. Though Pireaux et al. showed a similar tendency in their MO energy diagram obtained for shorter alkanes, methane to nonane, they did not distinguish between the $p\pi$ and σ_{2p} MOs, but labeled them together as MOs of the C 2p and H 1s character (or C 2p-derived MOs).[3] Figure 4, however, is more appropriate to interpret the spectra, because we can see the distributions of $p\pi$ and σ MO energies of longer *n*-alkanes separately. In particular, it is of note that the high density of states (DOS) around IP 11 eV is due to $p\pi$ MOs. On the other hand, the high DOS around 20 eV is ascribed to σ_{2s} MOs, which can be known from the diagram by Pireaux et al. as well. Another point to note is that there is no σ_{2p} MO but there are only $p\pi$ MOs near the bottom of the C 2p-derived MO region (just above the energy gap); the position of the lowest σ_{2p} MO is higher than the bottom of the C 2p-derived region by more than 1 eV for all the alkanes in Figure 4. Moreover, the IP values of the highest and lowest $p\pi$, the lowest σ_{2p}, and the highest σ_{2s} MOs remain almost constant irrespective of the number of carbons more than nine, although the highest occupied MO, which is of σ_{2p} character, tends to be more unstable. Consequently, it is reasonable to utilize these calculated results to assign the spectra of longer alkanes.

We now return to the experimental results and discuss them on the basis of the calculations. As mentioned before, films of different *n*-alkanes prepared under the same conditions give almost the same PIES as in Figure 2. Accordingly, it is confirmed experimentally by PIES that the valence electronic structure of a long-chain *n*-alkane is essentially unchanged regardless of chain length. Note that not only the electronic structure but also the orientation of surface molecules must be almost the same so that they are attacked by metastables at the same places and give the same PIES (see below).

Let us focus our attention on the spectra of $C_{44}H_{90}$ films, I_{44} and II_{44}. It will be shown below that the MO energy diagram

(28) The appearance of the substrate features in the UPS of film II_{44} is due to the nonuniformity of this film. See: Footnote 24.

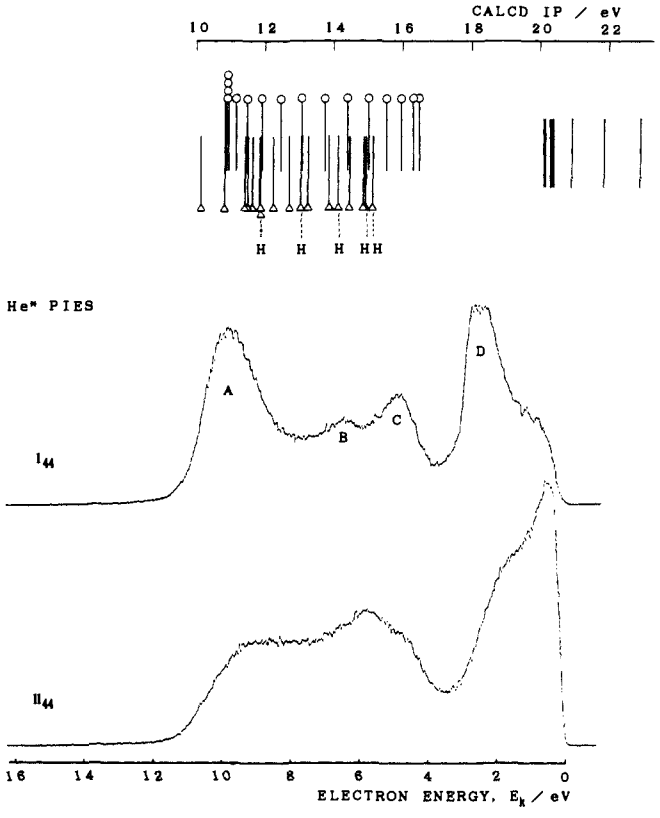

Figure 6. He* (2^3S, 19.82 eV) PIES of tetratetracontane films I_{44} (monolayer) and II_{44} (crystal). The calculated IP values for hexadecane are shown at the top of the figure. The IP scale is shifted so as to show a good agreement with the spectra. Bars labeled with open circles and triangles correspond to $p\pi$ and σ_{2p} MOs, respectively, the other bars to σ_{2s} MOs. The σ_{2p} MOs with large distribution on the terminal hydrogen atom are indicated by "H" in the energy diagram.

in Figure 4 well describes the spectral features and that the difference between the two spectra reflects different types of molecular aggregation. Since the angular distribution of Penning electrons is small compared to that of UPS,[29] it does not influence the following discussion. The PIES of the $C_{44}H_{90}$ films and the calculated IP values of $C_{16}H_{34}$ are compared in Figure 6. The IP scale is shifted so as to show a good agreement with the spectra. In the monolayer I_{44} spectrum, four bands A–D are observed; bands A and D are markedly enhanced and there is a deep hollow between bands C and D. Referring to the calculation, bands A and D are assigned to the high DOS of $p\pi$ and σ_{2s} MOs, respectively, whereas the hollow is ascribed to the energy gap. However, the high DOS of these MOs alone does not seem to be sufficient to explain the enhancement of the corresponding PIES bands. The enhancement of bands A and D is also attributable to the flat molecular orientation, because in this case metastables interact with $p\pi$ and σ_{2s} MOs extending perpendicularly to the carbon skeleton plane more effectively than with σ_{2p} MOs spreading along the plane (see Figure 7a). If the alkyl chain stood upright on the substrate surface (the case of film II_{44}; see below), $p\pi$ and σ_{2s} MOs would not be detected in the PIES, because metastables could not interact with the "sides" (methylene groups) of molecules, where $p\pi$ and σ_{2s} MOs are distributed (see Figure 7b). Though the enhancement of the band due to σ_{2s} MOs may seem rather strange at first sight since the constituent C 2s AOs are isotropic, the σ_{2s} MOs responsible for band D (those around IP 20 eV in the energy diagram) have a considerable contribution of H 1s AOs (see Figure 5) unlike the more stable MOs of the same type, which makes their shapes more favorable to be attacked by metastables effectively. On a graphite cleavage plane, planar molecules such as benzene,[30] pentacene,[16] and phthalocyanines[15,17]

(29) Conrad, H.; Ertl, G.; Küppers, J.; Sesselmann, W.; Haberland, H. *Surf. Sci.* **1982**, *121*, 161–180.

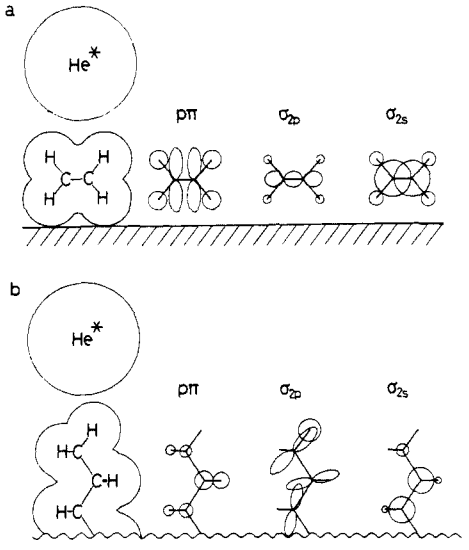

Figure 7. *n*-Alkane molecules interacting with metastable atoms in different molecular arrangements. (a) Flat-lying molecules in a monolayer, projected onto a plane perpendicular to the direction of the trans zigzag chain. Methyl groups are omitted. (b) Molecules standing upright in crystalline phase. From left to right, the van der Waals envelopes, $p\pi$, σ_{2p}, and σ_{2s} MOs are schematically shown.

lie flat on account of interaction between the π electrons of graphite and those of the molecules. Similarly, π (graphite)–$p\pi$ (alkane) interaction seems to orient the carbon skeleton plane of a *n*-alkane molecule parallel to the graphite surface. When the flat molecular orientation and the calculated energy of $p\pi$ MOs are taken into account, bands B and C are also assigned to $p\pi$ MOs. At present, however, we cannot explain why band B is observed in the energy region where no maximum of the DOS seems to exist, judging from the MO energy diagram. The relative intensity of bands B and C changes, depending on the amount of deposited *n*-alkane and also on the substrate temperature, although the intensities of bands A and D remain unchanged.[31,32]

In contrast, in the PIES of film II_{44} prepared on the copper substrate at room temperature (Figure 6), features corresponding to bands A–D of the monolayer are missing, which indicates $p\pi$ and σ_{2s} MOs are scarcely detected. Between electron energies (E_k) 6.5 and 5 eV, where the peaks of $p\pi$ bands B and C are located in the I_{44} spectrum, respectively, we can find a peak at E_k 6 eV. According to the calculation, the 1s AO of the terminal hydrogen atom within the carbon skeleton plane contributes appreciably to all the σ_{2p} MOs of $C_{16}H_{34}$ except for 58 and 56, shown in Figure 5. In particular, σ_{2p} MOs such as 54, 48, 43, 39, and 37 (indicated by "H" in the energy diagram of Figure 6) have very large distributions on the terminal hydrogen atom (see Figure 5). The last two of them exist near the bottom of the σ_{2p} MO region, with IPs smaller than that of the lowest $p\pi$ MO responsible for band C, by more than 1 eV. As a consequence, these MOs seem to be related to the 6-eV peak. If this is the case, other σ_{2p} MOs must also be responsible for the features in the spectrum of film II_{44}. When evaporated onto a metal substrate without a "clean" surface at room temperature, long-chain *n*-alkanes are known to form polycrystalline films with the trans zigzag chains perpendicular to the substrate surface.[5,9] In such films, σ_{2p} MOs protruding from the terminal hydrogen atom should be exclusively probed by metastables because the methyl end of a surface molecule is exposed outside. Therefore, the PIES features of film II_{44} are consistent with the molecular orientation in the crystalline film. From this fact together with another observation concerning

(30) Kubota, H.; Munakata, T.; Hirooka, T.; Kondow, T.; Kuchitsu, K.; Ohno, K.; Harada, Y. *Chem. Phys.* **1984**, *87*, 399–403.
(31) Ozaki, H.; Harada, Y., unpublished results.
(32) Nevertheless, the PIES of multilayers on graphite resemble those of the monolayers (films I) and are completely different from those of films II; *n*-alkanes do not form crystalline films on the graphite substrate as is the case for other organic compounds.[13]

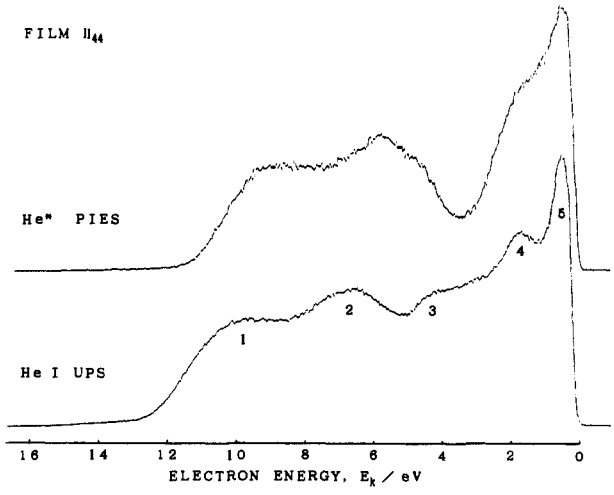

Figure 8. He* (2^3S, 19.82 eV) PIES and He I (21.22 eV) UPS of film II_{44}.

UPS (see below), we consider film II_{44} as crystalline, composed of *n*-alkane molecules standing upright. Similar PIES were obtained for other films with a "methyl surface": LB monolayer films formed on hydrophilic substrates[18,19] and zinc stearate films vapor-deposited on a stainless steel substrate at room temperature.[31]

As described before, the agreement between the electronic structure of long-chain *n*-alkane molecules reflected in the PIES and that obtained from MO calculations is fairly good. In other words, the DOS of each type MO shown in the energy diagram, modulated by its local electron distribution at the exposed molecular portion, can be surveyed experimentally by PIES. Conversely, it is noteworthy that the features of the valence electronic structure, especially the width of the C 2p-derived MO region and the relative position of the high DOS of the $p\pi$ MO, were reproduced qualitatively by the calculation even with the minimal basis.

In the UPS of the monolayer film I_{44} (Figure 3), where features due to the substrate are dominant, we can find neither a σ_{2s} band nor a hollow due to the energy gap, although three weak bands are observed in the C 2p-derived MO region (E_k > ca. 6 eV). The UPS of the crystalline film II_{44} is completely different from that of the monolayer even if the contribution of the substrate is subtracted from each spectrum. The difference is mainly ascribed to the features produced by secondary electrons in the crystalline film spectrum.[5,33] Among five bands 1–5, only band 1 is attributed to occupied MOs, while the others are ascribed to secondary electrons and are related to the electronic structure of unoccupied states (conduction bands). Secondary electrons produced by inelastic scattering of photoelectrons in the film accumulate at the high DOS of conduction bands to smear out spectral features due to occupied states ("valence bands").[5] As a matter of fact, conduction band features ("conduction bands") can be found also in the PIES, in which bands are essentially ascribed to occupied MOs.

The PIES and UPS of the crystalline film II_{44} are compared in Figure 8 in the E_k scale. Weak shoulders at 4.5 and 2 eV and a band at 0.5 eV of the PIES correspond to bands 3–5 of the UPS, respectively. The faint appearance of the "conduction bands" in the PIES is explained as follows. Since Penning ionization takes place at the outermost surface, and it is not an electron in an MO of a solid-phase molecule but an electron in the helium 2s AO that is ejected upon ionization (see Figure 1), the electronic structure of conduction bands should not be reflected directly in the PIES. Nonetheless, Penning electrons ejected on the surface with momenta directed to the inside of the surface penetrate into the film and undergo inelastic scattering to produce secondary electrons. When some of them are emitted, "conduction bands" will appear weakly in the PIES.

When the PIES of films I_{44} and II_{44} are compared in Figure 2, and the corresponding UPS of these films as well in Figure 3, no features due to secondary electrons are found in the PIES and UPS of film I_{44}. Namely, both spectra of the monolayer on graphite are almost free from the influence of secondary electrons. This effect is ascribable to little chance of scattering of photoelectrons or Penning electrons "in" the extremely thin film, the monolayer of flat-lying molecules, because these features appear as the film on graphite becomes thicker, as will be described in detail elsewhere. In previous work, "thick" polycrystalline films have been used as specimens for the photoelectron spectra of *n*-alkanes in solid phase and no "valence bands" except the first one have been observed with the He I resonance line, the other valence bands being obscured by secondary electrons.[5,33] In this case, higher energy light sources (He II resonance line[34] or synchrotron radiation[6]) are needed to obtain primary electron features in the UPS.

Conclusion

In the present work, the valence electronic structure of long-chain n-alkanes viewed with the MO picture was elucidated and the relation between the orientation of *n*-alkane molecules and the PIES was presented. The electronic structure is characterized by the high DOS of $p\pi$ and σ_{2s} MOs, which can be predominantly probed in the PIES of flat-lying molecules. In the PIES of molecules standing upright, on the contrary, σ_{2p} MOs with appreciable distribution on the terminal hydrogen atom are detected exclusively. In addition, in an ultrathin film of an organic compound such as a long-chain *n*-alkane forming a band structure in itself, Penning spectroscopy probes occupied orbitals selectively and, hence, unlike UPS, provides a spectrum almost free from the influence of conduction bands, making the interpretation of the spectrum simpler.

Acknowledgment. We thank Professor Kazuhiko Seki for his helpful discussion and Dr. Toshimasa Ishida for help in drawing the molecular orbitals.

Registry No. $C_{26}H_{54}$, 630-01-3; $C_{36}H_{74}$, 630-06-8; $C_{44}H_{90}$, 7098-22-8; $C_{10}H_{22}$, 124-18-5; $C_{13}H_{28}$, 629-50-5; $C_{16}H_{34}$, 544-76-3; $C_{19}H_{40}$, 629-92-5.

(33) Seki, K.; Ueno, N.; Sakamoto, K.; Hashimoto, S.; Sugita, K.; Inokuchi, H. *Rep. Prog. Polym. Phys. Jpn.* **1982**, *25*, 581–584.

(34) Seki, K.; Inokuchi, H. *Chem. Phys. Lett.* **1982**, *89*, 268–272.